Eur. Phys. J. D **10**, 225–231 (2000)

THE EUROPEAN PHYSICAL JOURNAL D

EDP Sciences

Vibrational resonances of non-rotating HCN in the excited $\tilde{A}^1A''$ electronic state

E. Soares Barbosa[1], R. McCarroll[1,a], T. Grozdanov[2], and P. Rosmus[3]

[1] Université Pierre et Marie Curie, Laboratoire de Dynamique des Ions, Atomes et Molécules[b], 75252 Paris Cedex 05, France
[2] Institute of Physics, P.O. Box 57, 11001 Belgrade, Yugoslavia
[3] Université de Marne-la-Vallée, Laboratoire de Chimie Théorique, 93166 Noisy-le-Grand, France

Received 27 July 1999 and Received in final form 18 October 1999

Abstract. A multi reference internally contracted configuration interaction (MRCI) method is used to generate the potential energy function (PEF) of the excited $\tilde{A}^1A''$ electronic state of HCN molecule. The analytic representation of the PEF is employed to calculate complex eigenvalues (resonance positions and widths) by a discrete variable representation (DVR) of the Hamiltonian for the non-rotating ($J = 0$) molecule. The computational method used is a variant of the filter-diagonalization technique based on a recursive polynomial expansion of the absorbing-boundary-conditions (ABC) Green operator. Reasonable agreement with existing experimental data is found.

PACS. 33.80.Gj Diffuse spectra; predissociation, photodissociation

1 Introduction

The classic experiment of Herzberg and Innes [1,2] on the VUV absorption bands of HCN and DCN around 190 nm has stimulated in the past, both semiempirical [3] and *ab initio* [4–10] theoretical studies of excited electronic states of HCN, as well as additional experimental work [11–14]. While experimentalists seem to be convinced [14] that all observed transitions can be assigned to a single excited $\tilde{A}^1A''$ state, theoreticians have repeatedly pointed out the importance of other nearby electronic states, especially the $2^1A'$ state [7,8]. Indeed, the predissociation, which has been observed [1] and later studied experimentally in more detail [12,13], indicates that coupling of two or more electronic states may be important for the full understanding of the photoabsorption dynamics. However, the knowledge of the excited electronic states and of the non-adiabatic couplings is far from being complete, so that one is necessarily forced to use various kinds of approximate treatments.

In the present paper we study the vibrational dynamics on the single adiabatic $\tilde{A}^1A''$ potential energy surface. Moreover, we shall limit ourselves to the geometries corresponding to the HCN isomer. To this end, *ab initio* electronic structure calculations on the level of multi reference internally contracted configuration interaction (MRCI) [26], have been performed in order to describe correctly the region of the HCN potential as well as the barrier separating it from the asymptotic dissociation limit H+CN($A^2\Pi$). The quasi-bound vibrational states (resonances) of the non-rotating ($J = 0$) molecule have then been calculated using the vibrational Hamiltonian in the discrete variable representation (DVR) [15]. The method used to find complex eigenvalues (positions and widths) of the resonances is a combination of ideas contained in previous works on filter-diagonalization [16], absorbing potentials [17,18] and Chebyshev polynomial expansions of the Green operator [19–21]. The method was originally proposed in reference [22] and later successfully applied to calculations of the vibrational resonances of ground-state molecules HCO [23], HO_2 [24] and H_3^+ [25].

In Section 2 we briefly describe our electronic structure calculations and discuss the main features of the potential energy function. Section 3 contains a description of the numerical method used to calculate complex eigenvalues of the quasi-bound states. Our results and discussion are presented in Section 4. Finally, Section 5 contains some concluding remarks.

2 Potential energy function

The three-dimensional adiabatic potential energy functions of the $X^1\Sigma^+$, $\tilde{A}^1A''$ and $\tilde{B}^1A'$ have been determined by extensive *ab initio* calculations. We have used the state averaged complete active space self-consistent field (CASSCF) approach with equal weights for all three states, with all valence molecular active orbitals. The CASSCF calculations were followed by an internally contracted multi reference configuration interaction (MRCI). The reference wave functions were selected according to a coefficient threshold of 0.01 in the CASSCF configuration expansion. All valence electrons were correlated. In all computations the spdf for C and N atoms and spd

[a] e-mail: ron@diam.jussieu.fr
[b] ESA 7066 du CNRS

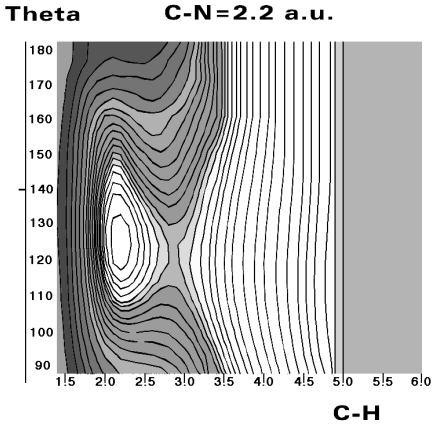

Fig. 1. Contour representation of the potential energy surface of the $\tilde{A}^1A''$ excited state of the HCN molecule as a function of $R_{\rm CH}$ and $\theta_{\rm HCN}$ for fixed value of $R_{\rm CN} = 2.2a_0$.

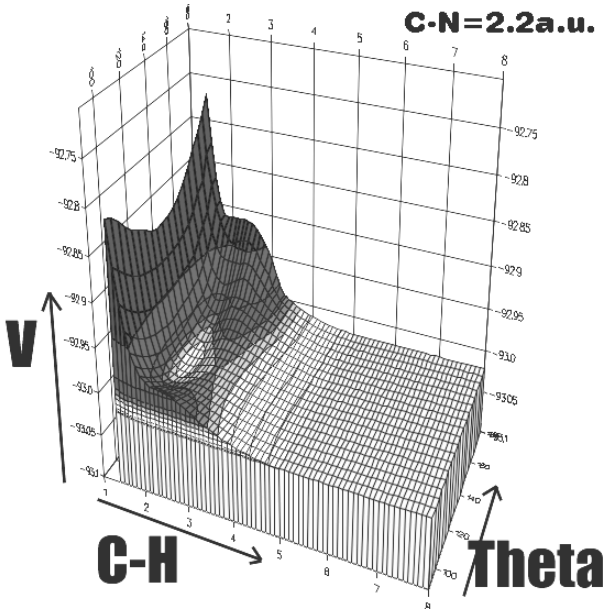

Fig. 2. 3D representation of the potential energy surface of the $\tilde{A}^1A''$ excited state of the HCN molecule as a function of $R_{\rm CH}$ and $\theta_{\rm HCN}$ for fixed value of $R_{\rm CN} = 2.2a_0$.

for H aug-cc-pVDZ basis of contracted Cartesian Gaussian functions of Dunning *et al.* [27] was employed. All electronic structure calculations were performed with the MOLPRO program package [26]. In the present contribution only the results related to the first electronically excited state of $\tilde{A}^1A''$ symmetry with a leading electronic configuration: $5(a')^26(a')^21(a'')7(a')$ correlating with the configuration: $5\sigma^21\pi^32\pi$ at linearity are presented. We have calculated about 500 *ab initio* points of the $\tilde{A}^1A''$ potential energy function. The distance $R_{\rm CH}$ varied from $1.4a_0$ to $8.0a_0$ with $\Delta R_{\rm CH} = 0.1a_0$, the distance $R_{\rm CN}$ varied between $1.8a_0$ to $3.0a_0$ with $\Delta R_{\rm CN} = 0.1a_0$, and the $\widehat{\rm HCN}$ angle $\theta_{\rm HCN}$ varied in the interval $[90°, 180°]$ with $\Delta\theta_{\rm HCN} = 5°$. Three one-dimensional polynomial interpolations were then used to obtain the potential energy function on a grid of about 16 500 points. The value of the potential energy function at any required point is then easily determined by a 3D spline fit. The analytic form can be obtained on request. The study of the non-adiabatic coupling effects for states forming conical intersections at near linear geometries have not yet been treated. We would expect however, that such a coupling does not influence the low lying predissociating vibrational states of the first electronically excited state of HCN.

Figure 1 shows a contour plot and Figure 2 a three-dimensional plot of the $\tilde{A}^1A''$ potential energy surface as a function of $R_{\rm CH}$ and $\theta_{\rm HCN}$ for fixed value of $R_{\rm CN} = 2.2a_0$. One can clearly distinguish the region of the HCN potential well, the region of the saddle point and the asymptotic region corresponding to H+CN($A^2\Pi$) dissociation limit. The minimum of the potential well $V_{\rm min} = -93.0367$ a.u. is located at $R_{\rm CHmin} = 2.1a_0$, $R_{\rm CNmin} = 2.47a_0$ and $\theta_{\rm HCNmin} = 123°$. These may be compare with the experiment values of Herzberg: $R_{\rm CHmin} = 2.154a_0$, $R_{\rm CNmin} = 2.4509a_0$ and $\theta_{\rm HCNmin} = 125°$. The saddle point, which was calculated to be 4398 cm^{-1} above the minimum corresponds to: $R_{\rm CHsaddle} = 3.0a_0$, $R_{\rm CNsaddle} = 2.38a_0$ and $\theta_{\rm HCNsaddle} = 123°$. Thus for energies less than the saddle point energy, dissociation is possible only through tunneling. In the asymptotic region starting from $R_{\rm CH}$ of about $5.0a_0$, we could also observe the $A^2\Pi$ CN potential energy function for all angular coordinates. The minimum of this asymptotic diatomic potential is 1561 cm^{-1} above the HCN minimum and corresponds to $R_{\rm CN} = 2.3a_0$.

We note also, that at linear geometries ($\theta_{\rm HCN} = 180°$), due to the existence of a conical intersection, the $\tilde{A}^1A''$ state correlates for small $R_{\rm CH}$ distances with the $1^1\Sigma^-$ state, while for large $R_{\rm CH}$ it correlates to one of the degenerate components of the $A^1\Pi$ singlet state (see, for example, [7]). In addition, near the bond angle $\theta_{\rm HCN} = 90°$ there is a pseudo-Jahn-Teller intersection [7,8] between the $\tilde{A}^1A''$ and B^1A' surfaces. In the present work, however, all non-adiabatic effects were neglected and the dynamics will be studied only on the single $\tilde{A}^1A''$ potential energy surface.

3 Selective calculation of resonances

Given the system Hamiltonian $\hat{H}$ one can introduce a complex absorbing potential iW (Re$W(R) \to \infty$ for the scattering coordinate $R \to \infty$) and consider the non-Hermitian operator:

$$\hat{H}(\lambda) = \hat{H} - {\rm i}\lambda\hat{W} \tag{3.1}$$

with a positive coupling strength λ. The coordinate dependent absorbing potential iW is usually taken to be non-zero only in the asymptotic region, where all physical interactions between the separated components of the system are zero. The resonances, which are rigorously defined as Siegert eigenvalues [28] or complex poles of the Green's function, could be obtained from the families of eigenvalues $Z_m(\lambda) = \epsilon_m - {\rm i}\Gamma_m/2$ of the Hamiltonian (3.1)

which converge to them as $\lambda \to 0$ [18]. Actually, for any finite basis representation an optimal value of λ exists which roughly corresponds to the stationary condition $\mathrm{d}Z_m(\lambda)/\mathrm{d}\lambda = 0$ (for more details see [17,18,23] and references therein).

Let us now describe the procedure of filter diagonalization, which generates a small-size basis appropriate for obtaining the eigenvalues in a given energy window: $E_{\min} < \mathrm{Re}Z_m(\lambda) < E_{\max}$. The essential idea [16,23] is to act with an operator function $f[E - \hat{H}(\lambda)]$ onto a generic initial wavepacket χ for a sequence of values $E_{\min} = E_1 < E_2 < ... < E_L = E_{\max}$:

$$\Psi_i = f[E_i - \hat{H}(\lambda)]\chi \; . \tag{3.2}$$

The operator function should be chosen in such a way that it filters out only the eigenstates from the initial wavepacket with eigenvalues close to E_i. In the case of bound states a very convenient choice [22,23] is the spectral density operator, *i.e.* $f(E-\hat{H}) = \mathrm{Im}\hat{G}^+ = \pi\delta(E-\hat{H})$. In any practical realization of this operator the Dirac delta-function is represented by a function of finite width which is highly peaked at the eigenvalues and hence acts as a filter. Generalizing this idea to the case of non-Hermitian Hamiltonian [23] we construct our window basis functions as:

$$\Psi_i = \mathrm{Im}\frac{1}{E_i - \hat{H}(\lambda)}\chi \; . \tag{3.3}$$

Taking χ to be real leads to the real Ψ_i's. It is quite obvious that the poles of the Green's function in (3.3) that are close in energy to an E_i will have a dominant contribution to the Ψ_i (see [23]); as such the small subspace of the window functions Ψ_i will represent the corresponding small eigensubspace of the $\hat{H}(\lambda)$.

In order to calculate the r.h.s. of (3.3) we apply the recursion expansion of the absorbing-boundary-conditions (ABC)Green operator [21,22] which enables generation of all the window functions simultaneously from the same iterative procedure. Namely, with the choice of the complex absorbing potential in the form

$$\hat{\mathrm{i}W} = \mathrm{i}\Delta H[\sin\varphi \sinh\hat{\gamma} + \mathrm{i}\cos\varphi(1 - \cosh\hat{\gamma})] \tag{3.4}$$

the following expansion has been proven to hold:

$$(E - \hat{H} + \mathrm{i}\hat{W})^{-1} = \frac{1}{\mathrm{i}\Delta H}\sum_{n=0}^{\infty}(2-\delta_{n0})\mathrm{e}^{-\mathrm{i}n\varphi} \times Q_n(\hat{H}_{\mathrm{norm}};\hat{\gamma})\,[\sin(\varphi - \mathrm{i}\hat{\gamma})]^{-1} \; . \tag{3.5}$$

The operators $Q_n(\hat{H}_{\mathrm{norm}};\hat{\gamma})$, $n = 0,1,2...$, are defined recursively as

$$Q_{n+1}(\hat{H}_{\mathrm{norm}};\hat{\gamma}) = \mathrm{e}^{-\hat{\gamma}}[2\hat{H}_{\mathrm{norm}}Q_n(\hat{H}_{\mathrm{norm}};\hat{\gamma}) - \mathrm{e}^{-\hat{\gamma}}Q_{n-1}(\hat{H}_{\mathrm{norm}};\hat{\gamma})] \; , \tag{3.6}$$

with the initial conditions

$$Q_0(\hat{H}_{\mathrm{norm}};\hat{\gamma}) = \hat{I} \; , \quad Q_1(\hat{H}_{\mathrm{norm}};\hat{\gamma}) = \mathrm{e}^{-\hat{\gamma}}\hat{H}_{\mathrm{norm}} \; . \tag{3.7}$$

Here $\hat{I}$ is the identity operator and the Hamiltonian $\hat{H}$ is scaled according to the formula

$$\hat{H}_{\mathrm{norm}} = \frac{\hat{H} - \bar{H}}{\Delta H} \; , \tag{3.8}$$

where $\bar{H} = (H_{\max} + H_{\min})/2$, $\Delta H = (H_{\max} - H_{\min})/2$, and $H_{\max}$ and $H_{\min}$ are respectively an upper and lower estimations of the maximum and minimum eigenvalues of the finite basis representation of the Hamiltonian $\hat{H}$, so that the spectral range of $\hat{H}_{\mathrm{norm}}$ belongs to $[-1,1]$.

The expansion of the Green operator defined by (3.5) has a desirable factorization of the energy dependence which comes through the phase φ as

$$\varphi = \arccos\left(\frac{E - \bar{H}}{\Delta H}\right) \; . \tag{3.9}$$

The dimensionless operator $\hat{\gamma}$ in (3.6) defines the damping factor $\mathrm{e}^{-\hat{\gamma}}$. In practice it should be chosen in accordance with the proper choice for the absorbing potential $\hat{W}$, which in turn has to be zero inside the strong interaction region and rise slowly in the asymptotic region where all the physical interactions are negligible. As such, in the application presented in Section 4, $\hat{\gamma}$ will be taken to be of the form

$$\gamma(R) = \begin{cases} 0 & R < R_1 \\ \gamma_0\left(\dfrac{R - R_1}{R_2 - R_1}\right)^2 & R_1 < R < R_2 \end{cases} \tag{3.10}$$

with γ_0 being the strength constant, and segment $[R_1, R_2]$ representing the asymptotic region of relevant radial coordinate.

In the $\hat{\gamma} \to 0$ limit the operators $Q_n(\hat{H}_{\mathrm{norm}};\hat{\gamma})$ tend to Chebyshev polynomials $T_n(\hat{H}_{\mathrm{norm}})$ and the relation (3.5) is converted into the known formal Chebyshev polynomial expansion of the Green operator $(E - \hat{H} + \mathrm{i}0+)^{-1}$ [19,20].

We now substitute (3.5) in (3.3), with additional restriction that the wavepacket χ has no overlap with the absorbing region where $\hat{\gamma} \neq 0$, so that

$$\frac{1}{\sin(\varphi - \mathrm{i}\hat{\gamma})}\chi = \frac{1}{\sin\varphi}\chi \; . \tag{3.11}$$

Our window basis functions defined by (3.3) then become

$$\Psi_{\mathrm{i}} = \frac{-1}{\Delta H \sin\varphi}\sum_{n=0}^{\infty}(2-\delta_{n0})\cos(n\varphi)\xi_n \; , \tag{3.12}$$

where the vectors ξ_n are given by the following three term recursion relation,

$$\xi_{n+1} = \mathrm{e}^{-\hat{\gamma}}[2\hat{H}_{\mathrm{norm}}\xi_n - \mathrm{e}^{-\hat{\gamma}}\xi_{n-1}]$$
$$\xi_0 = \chi \; , \xi_1 = \mathrm{e}^{-\hat{\gamma}}\hat{H}_{\mathrm{norm}}\xi_0. \tag{3.13}$$

After Schmidt orthogonalization and eventual elimination of the linear dependence among the functions Ψ_i, a final set of orthonormal window-basis functions $\bar{\Psi}_i$ ($i = 1,2,...\bar{L}, \bar{L} \leq L$) is obtained. This basis is then used to construct a small-size ($\bar{L} \times \bar{L}$) complex symmetric Hamiltonian matrix representing $\hat{H}(\lambda)$. Finally, this matrix is

then diagonalized by standard methods in order to obtain complex eigenvalues with real parts in the desired energy window $[E_{\min}, E_{\max}]$.

We note that, as defined by relation (3.4), our effective absorbing potential is energy-dependent $\hat{\imath}W = \hat{\imath}W(E)$. However, the width of the energy window $E_{\max} - E_{\min}$ is much smaller than the spectral range ΔH, so that this dependence is effectively reduced. Namely, for each energy window the midpoint energy $\bar{E} = (E_{\max}+E_{\min})/2$, can be chosen to define the energy independent absorbing potential $W(\bar{E})$ to be used in the construction of the complex Hamiltonian matrix.

Strictly speaking, the recursion procedure, as it is defined above, generates a basis appropriate for diagonalization of the Hamiltonian $\hat{H}(\lambda = 1)$, while the strength of the absorbing potential is defined by the parameter γ_0 of the damping potential (3.10). Therefore, one would have to perform many expensive calculations for different γ_0's in order to determine the optimal parameter $\bar{\gamma}_0$ from a stationary condition: $\mathrm{d}Z_m/\mathrm{d}\gamma_0|_{\gamma_0=\bar{\gamma}_0} \approx 0$. Instead, it is much more efficient to consider a family of complex Hamiltonians $\hat{H}(\lambda) = \hat{H} - \mathrm{i}\lambda W(\bar{E})$. After a small window basis is obtained for some reasonable γ_0, a series of diagonalizations for various values of λ around $\lambda = 1$ can be performed using the same basis. The optimal values of λ can than be determined by looking for stationary points on the trajectories $Z_m(\lambda)$ in the complex energy plane. This procedure greatly reduces numerical effort in finding optimized resonance parameters.

4 Computational details and results

The vibrational Hamiltonian of the non-rotating ($J = 0$) HCN molecule in atom-diatom Jacobi coordinates is

$$\hat{H} = \frac{-\hbar^2}{2m_{\mathrm{H,CN}}}\frac{1}{R}\frac{\partial^2}{\partial R^2}R - \frac{\hbar^2}{2m_{\mathrm{CN}}}\frac{1}{r}\frac{\partial^2}{\partial r^2}r + \frac{\hbar^2}{2}\left(\frac{1}{m_{\mathrm{H,CN}}R^2} + \frac{1}{m_{\mathrm{CN}}r^2}\right)\hat{\mathbf{j}}^2 + V(R,r,\theta) \quad (4.1)$$

where R is the radial distance from H to the center of mass of CN; r is the CN internuclear distance; θ is the angle between $\mathbf{R}$ and $\mathbf{r}$; $\hat{\mathbf{j}}$ is the CN angular momentum operator and $m_{\mathrm{H,CN}}$ and m_{CN} are the usual reduced masses.

The Hamiltonian (4.1), the complex absorbing potential (3.4), and the damping potential (3.10) are represented in a DVR basis.

The basis set parameters corresponding to the main calculation are the following.

- For R (the dissociation coordinate) we used $N_R = 80$ equidistant sinc-function DVR [29,30] points in the interval $[1.7, 9]a_0$.
- For the r coordinate we used $N_r = 70$ sinc-function DVR points in the interval $[1.8, 3]a_0$.
- For the angular variable we used $N_\theta = 80$ Gauss-Legendre-quadrature DVR points.

The direct product basis of size $N_R \times N_r \times N_\theta = 448\,000$ is further contracted by retaining only grid points which represent the potential surface in the available range of internal coordinates: $1.4a_0 < R_{\mathrm{CH}} < 8a_0$, $90^\circ < \theta < 180^\circ$ and in addition satisfy the cutoff criterion $V(R,r,\theta) < V_{\mathrm{cut}} = 40\,000\ \mathrm{cm}^{-1}$ (the zero of energy is set at the minimum of the HCN potential well). The number of DVR points, surviving after the cutoff procedure was $N_{\mathrm{DVR}} \sim 150\,000$. The damping potential has been taken in the form of (3.10) with $R = R_{\mathrm{CH}}$, $R_{\mathrm{CH1}} = 5a_0$, $R_{\mathrm{CH2}} = 8a_0$ and various values of γ_0 around $\gamma_0 = 0.05$.

For the most time consuming computational part in the iterative procedure, the matrix-vector multiplication, we used an algorithm which takes advantage of the sparseness of the DVR Hamiltonian, similar to the one described in reference [30]

Many test calculations corresponding to different basis set parameters $N_{\mathrm{DVR}}, V_{\mathrm{cut}}$ and γ_0 were carried out in order to assure that the results obtained were converged to better than 1 cm^{-1} for the positions and about 20% for the widths for most resonances.

In order to cover the energy interval of interest, three overlapping energy windows: $[0, 4000]$, $[3000, 6000]$ and $[5000, 8000]$ cm^{-1} have been used with around 100 window basis functions (3.12) in each of them. The number of iterations needed for obtaining the above stated degree of convergence was 10 000. Each calculation required about 3 hours CPU time on a IBM RS 6000 workstation.

After a window basis is generated and Schmidt orthogonalized a parametric family of complex-symmetric Hamiltonians $\hat{H}(\lambda)$ defined by (3.1) is diagonalized yielding a set of trajectories $Z_m(\lambda)$ in the complex energy plain. This last step takes typically less than 1% of total CPU time.

The trajectories $Z_m(\lambda)$ are drawn in the complex energy plane. For a given trajectory a stationary point (typically corresponding to a cusp or to a center of the maximum curvature of a loop) is used to extract the resonance parameters. Two examples are shown in Figures 3 and 4.

Results of calculations are given in Table 1. The assignments (v_1, v_2, v_3) in terms of the harmonic quantum numbers in the CH stretch, the HCN bend and the CN stretch are tentative for higher states. In particular, doubts might be raised about our assignment of the $(0, 5, 0)$ state. The accuracy of our calculations for $(0, n, 0)$ series deteriorates progressively with n. So it is a little surprising that a difference between theory and experiment is much smaller for $n = 5$ than for $n = 3$ or 4. We do not believe that this to be of great significance. It is possible that non adiabatic effects, which are not taken account of in the present calculations, might affect the $(0, 5, 0)$ and more highly excited states. Also listed are the positions of levels as derived from experimental data [1] on $\tilde{A}(0, v_2, v_3)^1 - \tilde{X}(0, 0^0, 0)$ transitions. Reasonable agreement is found between the calculated resonance positions (real parts of the complex eigenvalues) and experimental data corresponding to $(0, v_2, 0)$ and $(0, v_2, 1)$ progressions. The resonance widths (imaginary parts of the complex eigenvalues) of these quasi-bound states is also in

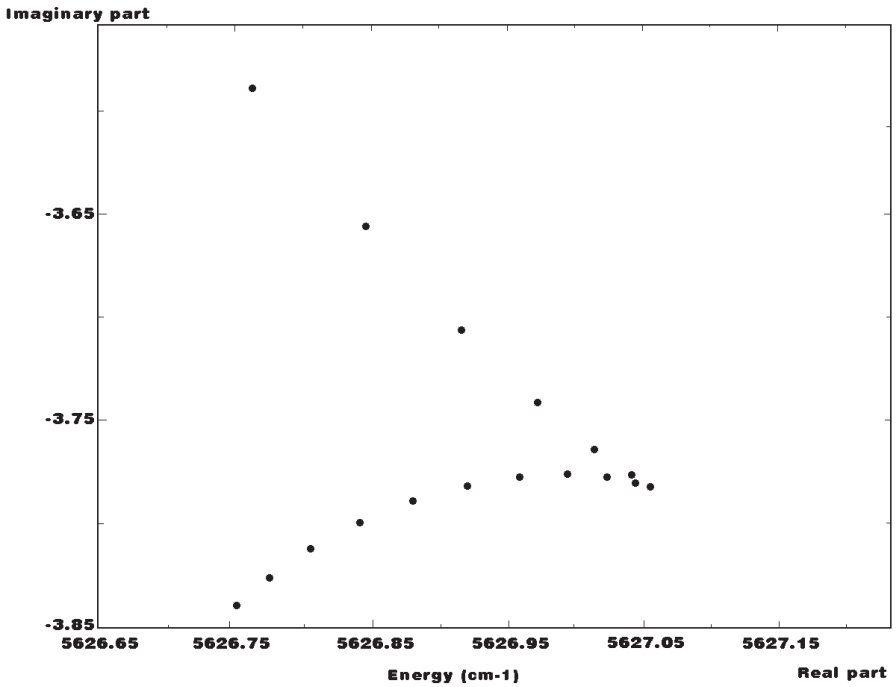

Fig. 3. Trajectory $Z(\lambda)$ of a complex eigenvalue of Hamiltonian (3.1). The location of the $(1,1,0)$ resonance corresponds to the cusp point.

Table 1. Real (ReE) and imaginary (ImE) parts of resonance eigenvalues (in cm^{-1}) of the non-rotating ($J = 0$) HCN molecule in $\tilde{A}^1A''$ state. The real parts (resonance positions) are shown relative to the position of $(0,0,0)$ state at 2560.95 cm^{-1} above the minimum of the $\tilde{A}^1A''$ potential. Experimental values for the positions (EXP) are from reference [1]. Quantum numbers (v_1, v_2, v_3) correspond to HC stretch, the bend and CN stretch. $A.B(-C)$ stands for $A.B \times 10^{-C}$.

state	(v_1, v_2, v_3)	ReE	ImE	EXP
1	$(0,0,0)$	0	$-9.23(-8)$	0
2	$(0,1,0)$	948.7	$-9.78(-6)$	938
3	$(0,0,1)$	1497.5	$-1.17(-3)$	1493
4	$(0,2,0)$	1891.3	$-6.68(-4)$	1858
5	$(1,0,0)$	2222.3	-0.688	
6	$(0,1,1)$	2431.4	-0.120	2428
7	$(0,3,0)$	2823.7	$-4.52(-2)$	2755
8	$(0,0,2)$	2981.0	-0.393	
9	$(1,1,0)$	3066.1	-3.78	
10	$(0,2,1)$	3356.7	-0.829	3342
11	$(0,4,0)$	3771.2	-4.52	3626
12	$(1,0,1)$	3857.8	-42.5	
13	$(0,1,2)$	3904.1	-67.1	
14	$(1,2,0)$	3942.1	-8.25	
15	$(0,3,1)$	4281.3	-5.25	4233
16	$(0,5,0)$	4453.0	-1.17	4460
17		4628.2	-49.1	
18		4742.0	-50.4	
19		4796.7	-19.5	
20		4861.4	-8.85	
21		5190.0	-38.7	
22		5240.8	-19.2	
23		5371.0	-14.3	

qualitative agreement with findings of reference [1] where the exceptional stability of the $(0, v_2, 0)$ states was observed.

Table 2 shows a comparison between different experiments and calculations for the fundamental transitions. The present anharmonic wavenumbers are found to be in a good agreement with the experimental data for the bending and CN stretching. We have obtained the following wavenumbers $\tilde{\nu}_2 = 948$ cm^{-1} $\in [940, 959]$ and $\tilde{\nu}_3 = 1497$ cm^{-1} $\in [1493, 1506]$. However, an estimation of the $\tilde{\nu}_1 = 3160$ cm^{-1} frequency by Innes and Bickel based on the DCN isotope measurements is not supported by the present calculations, which give $\tilde{\nu}_1 = 2222$ cm^{-1}. The two reported theoretical calculations, based on a three dimensional potential energy functions [6,10] yield $\tilde{\nu}_1 = 2351$ cm^{-1} and $\tilde{\nu}_1 = 2144$ cm^{-1} which are relatively close to our result. Obviously the energy of this level is strongly influenced by the shape and height of the barrier along the dissociation path.

Our calculations predict that state $(1,0,0)$ is relatively stable in spite the fact that it has not been observed in experiments [1]. Possible reasons could be unfavorable Franck-Condon factors and/or presence of other predissociation mechanisms.

In the experimental work [12] the radiative lifetimes of the states corresponding to low-J components of the $(0,1,0)^0$ and $(0,2,0)^0$ levels have been measured to be, respectively 136 ns and 9 ns. These values correspond to imaginary parts of complex energies of 1.9×10^{-5} cm^{-1} and 6.6×10^{-4} cm^{-1}, which are, especially in the second case, in fairly good agreement with our results from Table 1. We note however, that authors of reference [12] tentatively assigned the measured lifetimes to different predissociation mechanisms including also the spin-orbit coupling with the $1^3A'$ state.

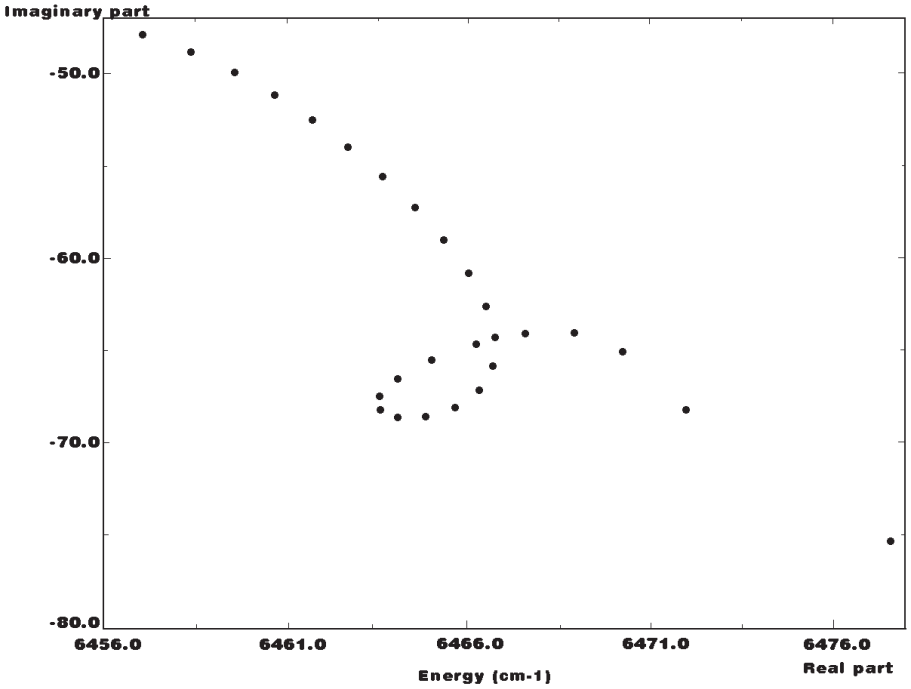

Fig. 4. Trajectory $Z(\lambda)$ of a complex eigenvalue of Hamiltonian (3.1). The location of the $(0, 1, 2)$ resonance corresponds to the center of the highest curvature on the loop.

Table 2. Comparison between experiments and various calculations of anharmonic vibrational wavenumbers (in cm^{-1}). c_1: one-dimensional analysis (Peric *et al.*) [7,8]; c_2: two-dimensional analysis (Peric *et al.*) [7,8]; c_3: CISD potential with 92 CI (Schaefer) [6]; c_4: CISD potential+Davidson correction (Schaefer) [6]; c_5: MRCI potential (Botschwina *et al.*) [10]; e_1: experiment: analysis from DCN (Bickel and Innes) [11]; e_2: experiment: abstract of the original paper by Herzberg [1]; e_3: experiment: Herzberg [2].

state	c_1	c_2	c_3	c_4	c_5	e_1	e_2	e_3	our calculation
(010)		1030	976	954	956	959	949	940.6	948
(001)	1700	1675	1596	1507	1497	1520	1506	1495	1497
(100)	2435	2300	2478	2351	2144	3160			2222

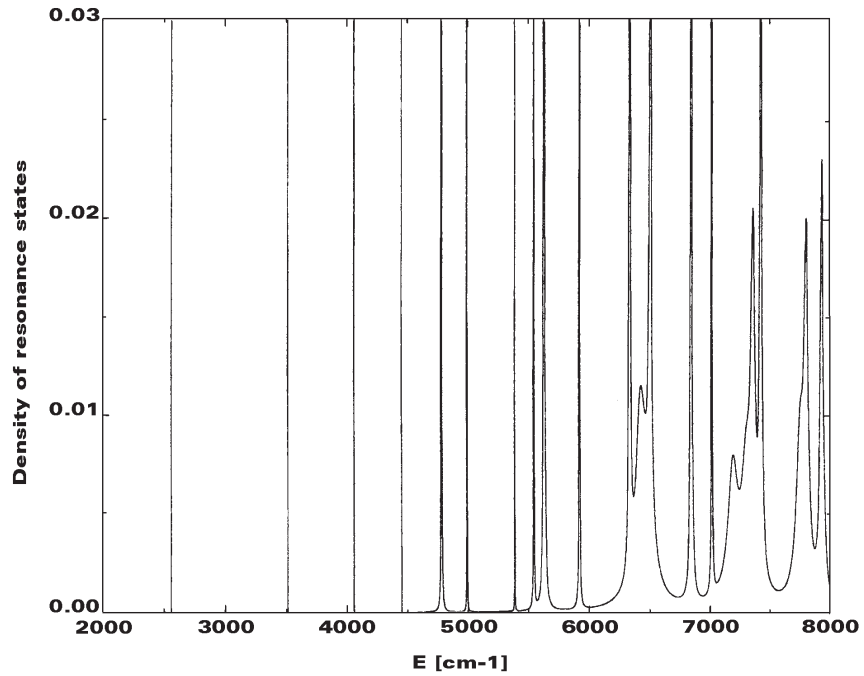

Fig. 5. The density of resonance states obtained from the data in Table 1 using the equation (4.2).

Having calculated the resonance poles, the resonance density of states can be constructed by summing over these poles and assuming the Lorentzian contributions:

$$\rho(E) = \sum_n \frac{\Gamma_n/2\pi}{(E-\epsilon_n)^2 + \Gamma_n^2/4} \cdot \qquad (4.2)$$

Figure 5 shows the resonance density of states obtained by using data from Table 1 and equation (4.2).

5 Conclusion

For highly excited quasi-bound states, the accuracy of the results may be affected by our neglect of possible tunneling to the HNC isomer and non-adiabatic coupling with the higher electronic states. However the present results for the low lying quasi-bound states of HCN in the excited electronic state $\tilde{A}^1A''$ are in a good agreement with experiments and confirm the validity of the approximations used, the accuracy of the potential energy function and the efficiency of the dynamical method.

The variant of the filter diagonalization method used, which includes the complex absorbing potentials and recursive polynomial expansion techniques, has proved to be successful in treating predissociative dynamics of non-linear triatomic systems. As in previous applications [23–25], this method provides precise resonance positions and reasonably good estimates of the resonance widths. It can be easily generalized to treat additional degrees of freedom, such as for example, rotating triatomics or polyatomic molecules.

This work was supported by the IDRIS (Institut du Développement et des Ressources en Informatique Scientifique) center and the CCR (Centre de Calcul de Recherche de Jussieu). E. Soares Barbosa wishes also to thank Reinhard Schinke for a very stimulating stay in his group and for many fruitful discussions concerning the fits of the potential energy functions.

References

1. G. Herzberg, K.K. Innes, Can. J. Phys. **35**, 842 (1957).
2. G. Herzberg, *Electronic spectra of polyatomic molecules* (Van Nostrand, Princeton, 1966).
3. S.C. Ross, P.R. Bunker, J. Mol. Spectrosc. **105**, 369 (1984).
4. G.M. Schwenzer, S.V. O'Neil, H.F. Schaefer, C.P. Baskin, C.F Bender, J. Chem. Phys. **60**, 2787 (1974).
5. L.C. Lee, J. Chem. Phys. **72**, 6414 (1980).
6. W.D. Laidig, Y. Yamaguchi, H.F. Schaefer, J. Chem. Phys. **80**, 3069 (1984).
7. M. Peric, H. Dohman, S.D. Peyerimoff, R.J. Buenker, Z. Phys. D. **5**, 65 (1987).
8. M. Peric, R.J. Buenker, S.D. Peyerimoff, Mol. Phys. **64**, 843 (1988).
9. J.F. Stanton, J. Gauss, J. Chem. Phys. **100**, 4695 (1994).
10. P. Botschwina, M. Horn, M. Matuschewski, E. Schick, P. Sebald, J. Mol. Struct. Theochem **400**, 119 (1997).
11. G.A. Bickel, K.K. Innes, Can. J. Phys. **62**, 1763 (1984).
12. Y.-C. Hsu, M.A. Smith, S.C. Wallace, Chem. Phys. Lett. **111**, 219 (1984).
13. A. Meenakshi, K.K. Innes, J. Chem. Phys. **84**, 6550 (1986).
14. A. Meenakshi, K.K. Innes, G.A. Bickel, Mol. Phys. **68**, 79 (1989).
15. J.C. Light, I.P. Hamilton, J.V. Lill, J. Chem. Phys. **82**, 1400 (1985).
16. D. Neuhauser, J. Chem. Phys. **93**, 2611 (1990); *ibid.* **95**, 4927 (1991); *ibid.* **100**, 5076 (1994); M.R. Wall, D. Neuhauser, J. Chem. Phys. **102**, 8011 (1995).
17. G. Jolicard, E.J. Austin, Chem. Phys. Lett. **121**, 106 (1985); Chem. Phys. **103**, 295 (1986); G. Jolicard, C. Leforestier, E.J. Austin, J. Chem. Phys. **88**, 1026 (1988).
18. U.V. Riss, H.-D. Meyer, J. Phys. B **26**, 4503 (1993).
19. R. Kosloff, J. Phys. Chem. **92**, 2087 (1988); B. Hartke, R. Kosloff, S. Ruhman, Chem. Phys. Lett. **158**, 238 (1989).
20. Y. Huang, W. Zhu, D.J. Kouri, D.K. Hoffman, Chem. Phys. Lett. **206**, 96 (1993).
21. V.A. Mandelshtam, H.S. Taylor, J. Chem. Phys. **103**, 22 (1995).
22. V.A. Mandelshtam, H.S. Taylor, J. Chem. Phys. **102**, 7390 (1995).
23. T.P. Grozdanov, V.A. Mandelshtam, H.S. Taylor, J. Chem. Phys. **103**, 7990 (1995).
24. V.A. Mandelshtam, T.P. Grozdanov, H.S. Taylor, J. Chem. Phys. **103**, 10074 (1995).
25. V.A. Mandelshtam, H.S. Taylor, J. Chem. Soc. Far. Trans. **93**, 847 (1997).
26. MOLPRO is a package of *ab initio* programs written by H.-J. Werner and P.J. Knowles with contributions from R.D. Amos, A. Berning, D.L. Cooper, M.J.O. Deegan, A.J. Dobbyn, F. Eckert, C. Hampel, T. Leininger, R. Lindh, A.W. Loyd, W. Meyer, M.E. Mura, A. Nicklaß, P. Palmieri, K. Peterson, R; Pitzer, P. Pulay, G. Rauhut, M. Shütz, H. Stoll, A.J. Stone and T. Thorsteinsson; further details at `http://www.tcbham.ac.uk/molpro`.
27. T.H. Dunning Jr, J. Chem. Phys. **90**, 1007 (1989); D.E. Woon, T.H. Dunning Jr, J. Chem. Phys. **98**, 1358 (1993).
28. L.D. Landau, E.M. Lifshitz, *Quantum Mechanics* (Pergamon, London, 1958), pp. 440-441.
29. D.T. Colbert, W.H. Miller, J. Chem. Phys. **96**, 1982 (1992).
30. G.C. Groenenboom, D.T. Colbert, J. Chem. Phys. **99**, 9681 (1993).